Nuclear Deflection of Potentially Hazardous Objects as a Function of Burst Height, Device Yield, and Object Composition.

Catherine S. Plesko and Walter F. Huebner

with special thanks to the LANL EAP and MCNP Project Teams

Los Alamos National Laboratory and Southwest Research Institute

15 May, 2013

Physical Processes Involved in Hazard Mitigation by Stand-Off Nuclear Burst

Energy Deposition

↓

Material Response

↓

Bulk Object Response

A Multi-Dimensional Problem Space

- Open questions for fast push mitigation in general:
  - PHO physical characteristics
  - Energy coupling—how much Δv from a given yield?
- Variables for each mitigation attempt:
  - Size of object
  - Composition of object
    (Fe-Ni, stony, carbonaceous, cometary)
  - Structure
    (monolithic, fractured, rubble pile)
  - Shape
  - Warning time
  - Trajectory

An Overview of Nuclear Device Physics

- Fissile material, hydrogen compressed, energy is released.
- Multiple pathways for energy release:
  - Thermal and Kinetic: $\approx 97\%$ yield
  - Nuclear radiation (γ-rays, neutrons): $\approx 3\%$ yield

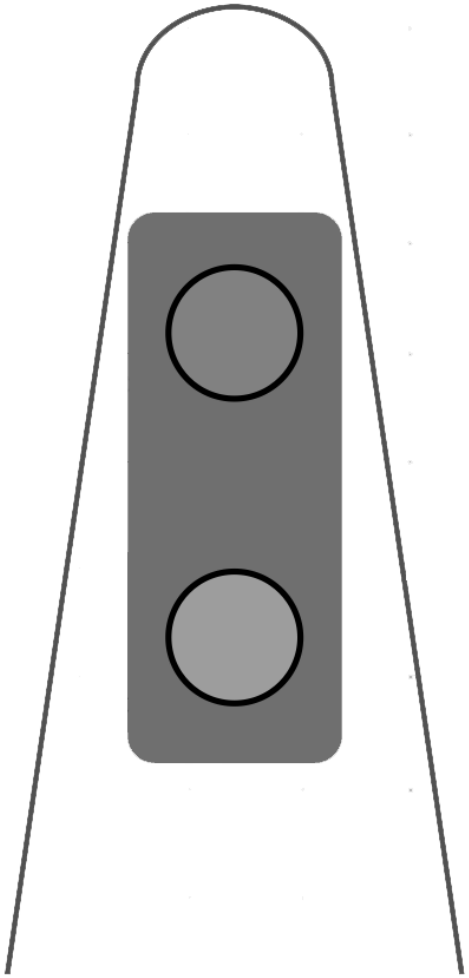

Energy Deposition by Neutrons and γ-rays

- Particle-like
- γ's: ≈ 10 cm
- Neutron energy deposition
  - scattering
  - capture
  - scales linearly in density
  - crystal structure, porosity irrelevant
- Deposited before hydrodynamic response
- Energy, $E(\vec{x})$, calculated in a particle transport code
- ENDF Libraries: www.nndc.bnl.gov, Chadwick et al. (2006)

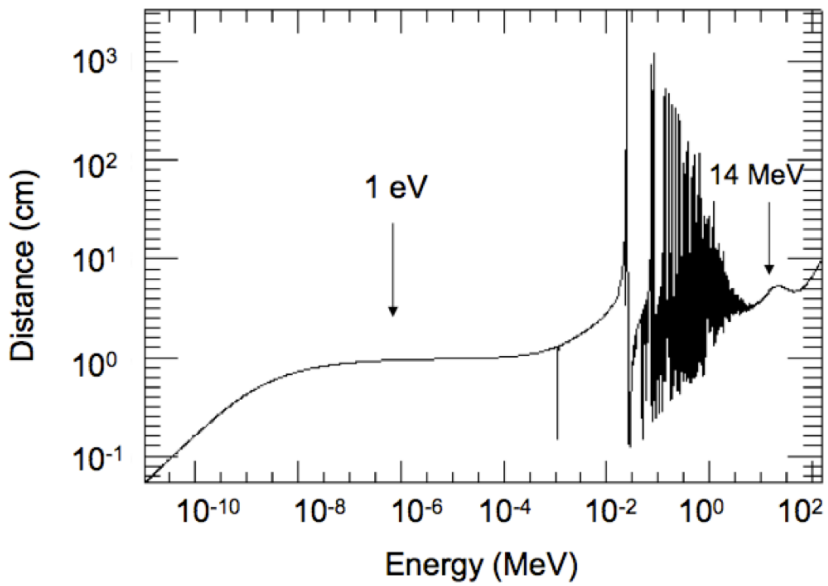

Mean free path of neutrons in iron, by energy.

Neutron-Mediated Nuclear Reactions

n^0 Scattering

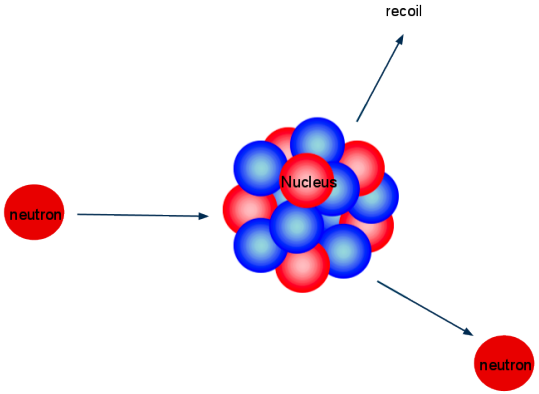

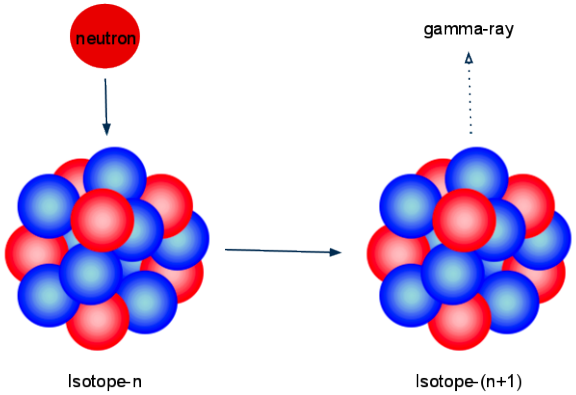

$^{n}X(n,\gamma)^{n+1}X$

$^{n}_{m}X(n,\alpha)^{(n-4)}_{(m-2)}X$

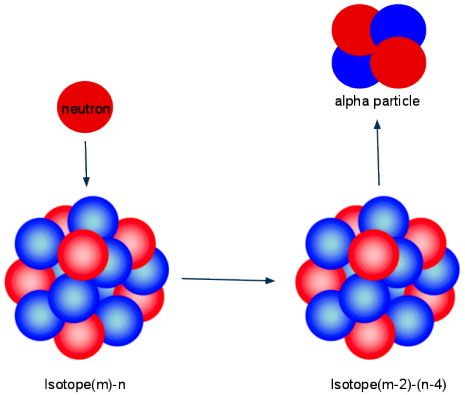

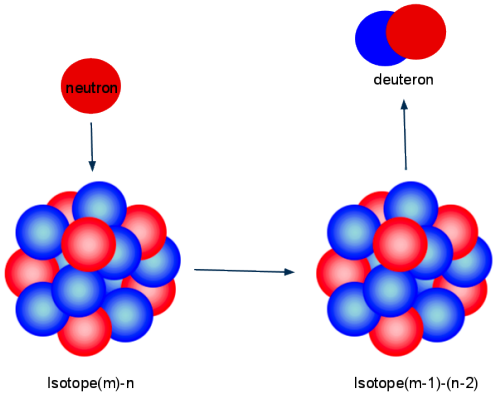

$^{n}_{m}X(n,d)^{(n-2)}_{(m-1)}X$

Neutron Cross Sections in Meteoritic Materials

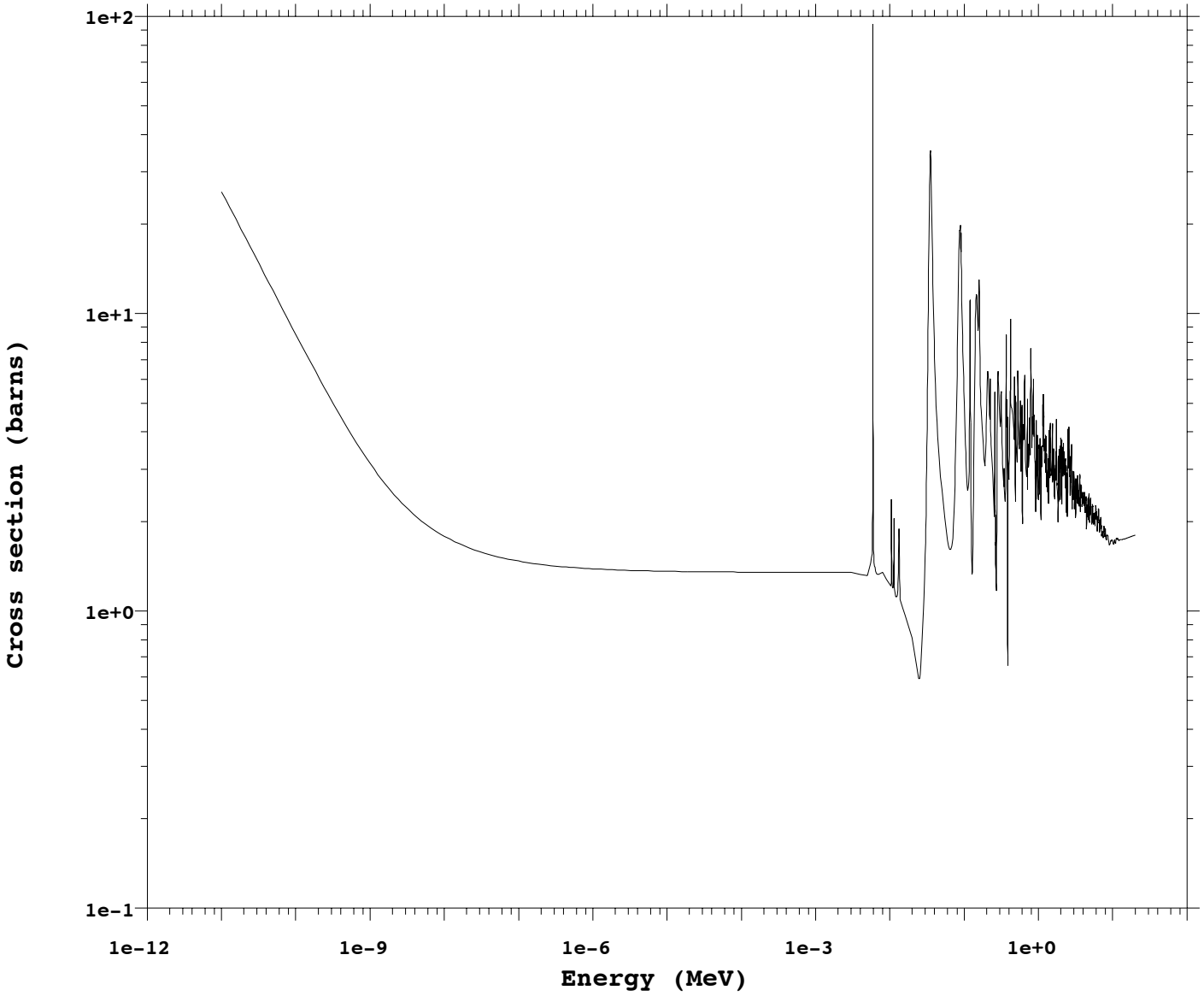

Carbon

Neutron Cross Sections in Meteoritic Materials

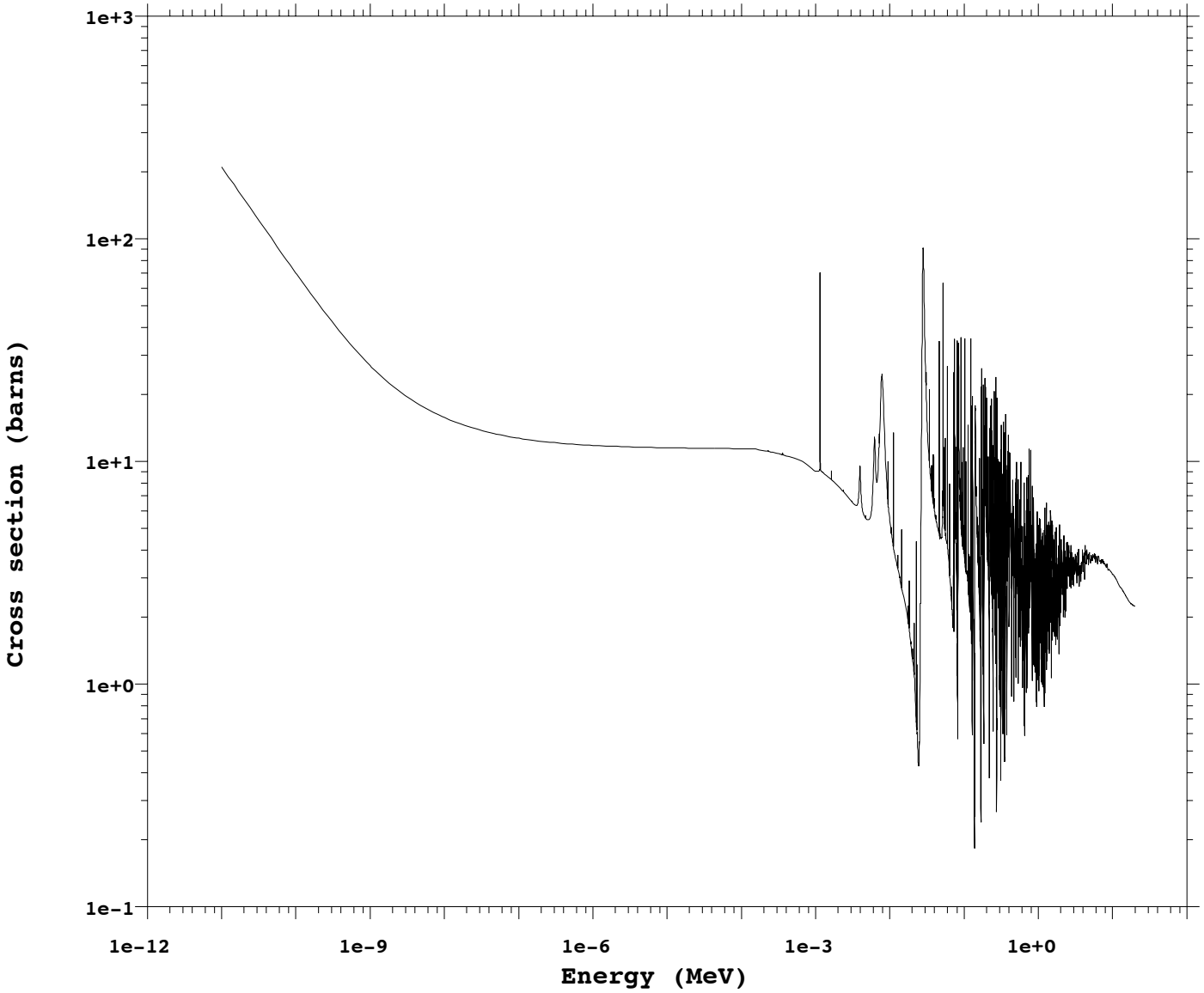

Iron

Neutron Cross Sections in Meteoritic Materials

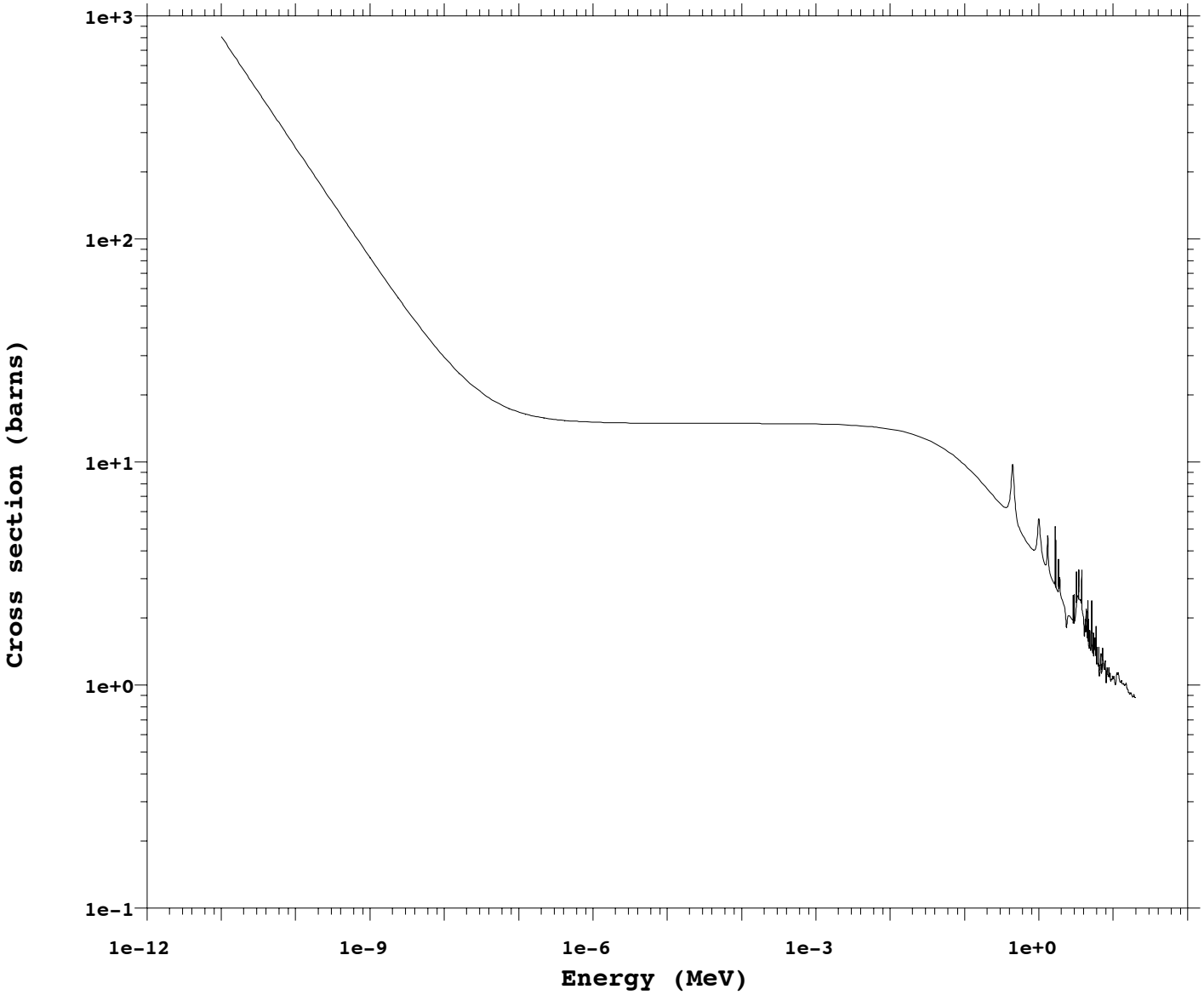

H_2O

Neutron Cross Sections in Meteoritic Materials

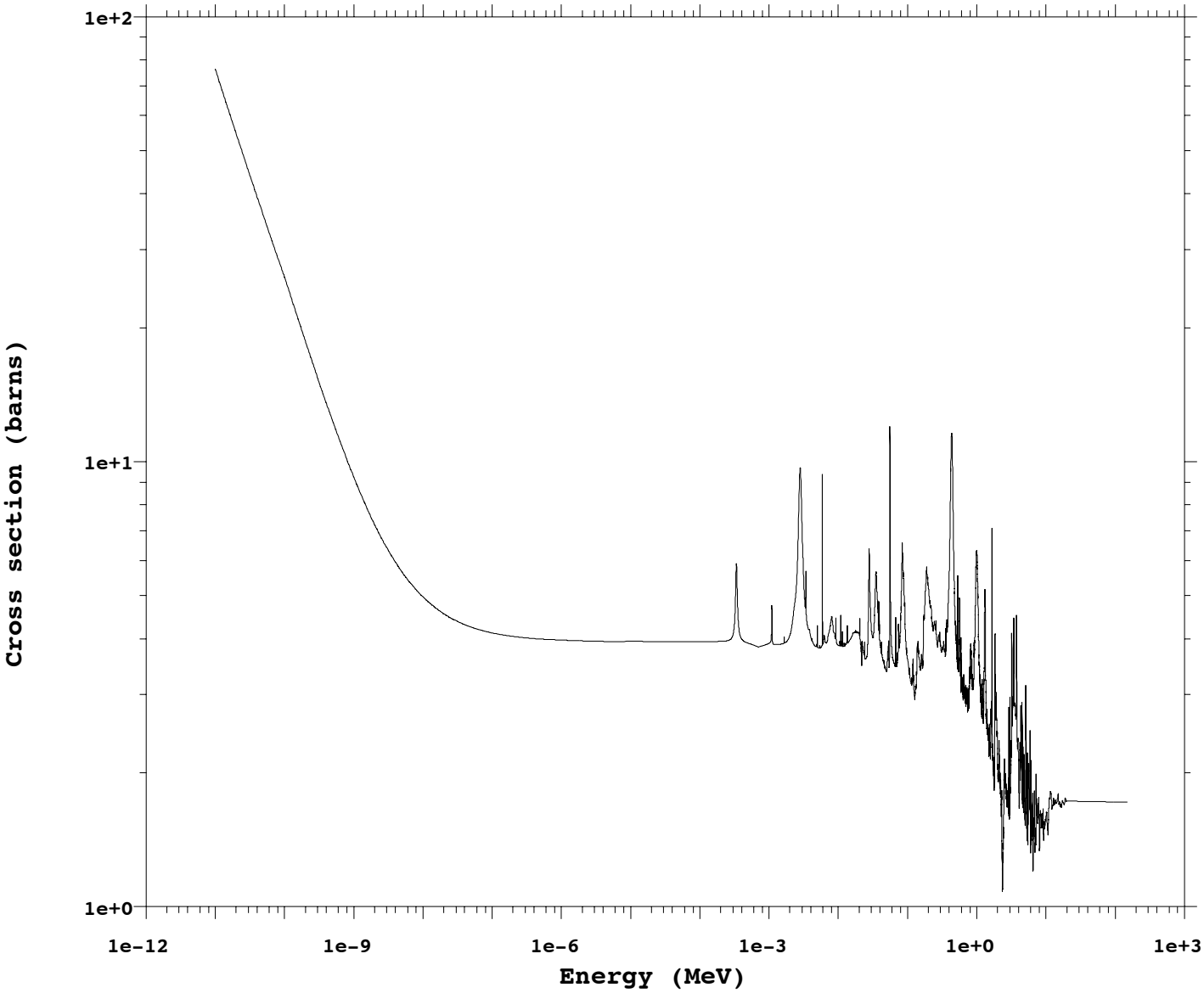

Basalt, Barnes and Lyon (1988)

Neutron Cross Sections in Meteoritic Materials

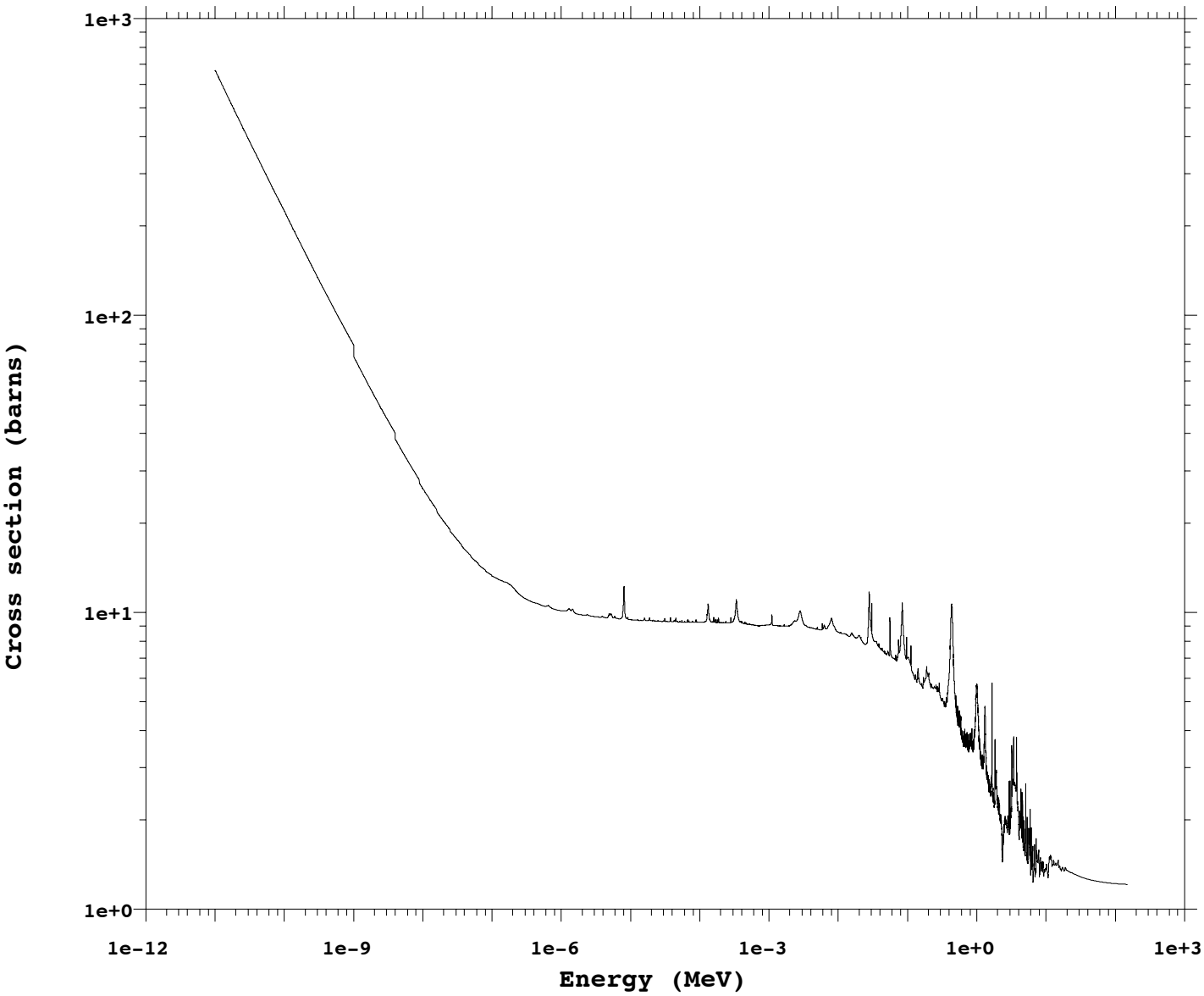

CI-Chondrite, Lodders (2003)

The Monte Carlo N-Particle Transport Code (MCNP)

- Propagation of particles, including n^0, γ-rays, e^-.
- Cumulative statistics of many individual stochastic processes.
- Including: n^0 scatter, capture, fission, photon production, capture, etc.

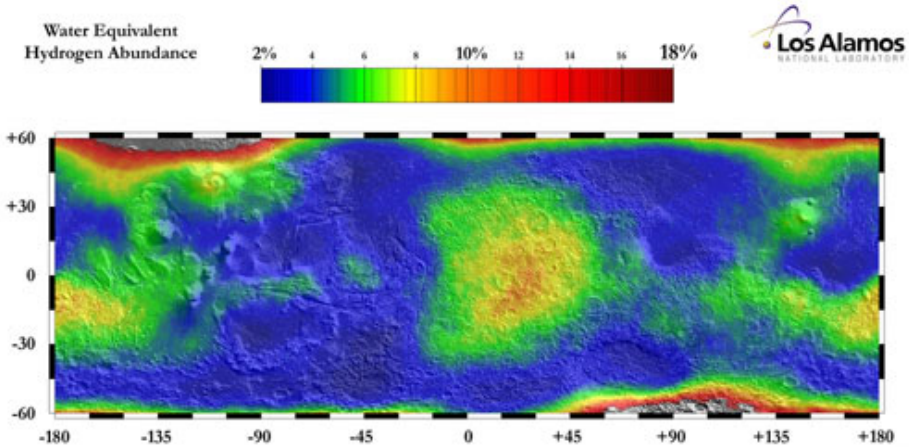

MCNP used to model H in Martian soil from Mars Odyssey data.

Prettyman et al. (2004), Feldman et al. (2002).

MCNP Slab Model Geometry

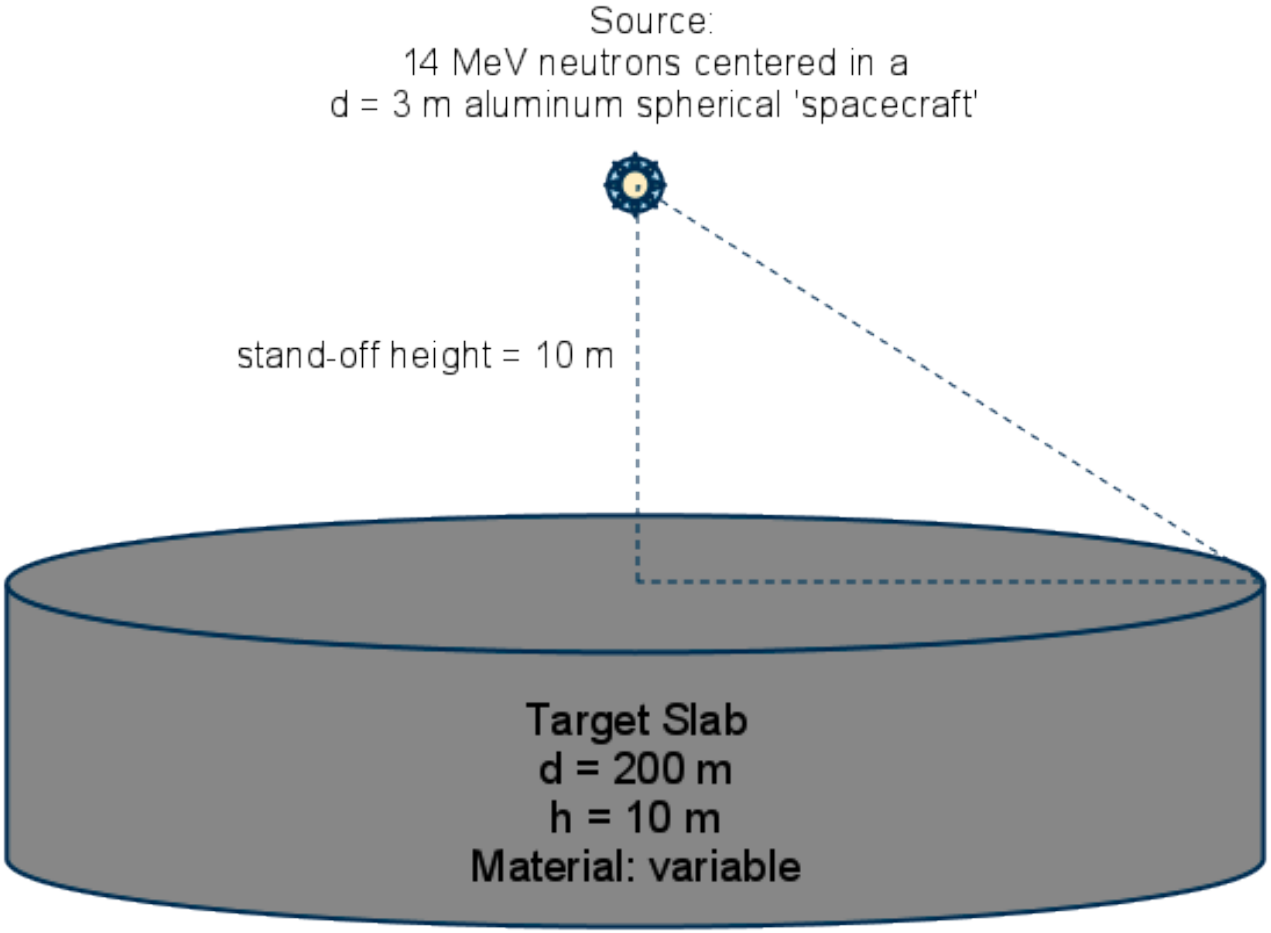

- Statistical resolution: 300 million particles
- Mesh resolution: 1 cm x 1 cm x 1 degree

MCNP Slab Model Particle Energy Distribution

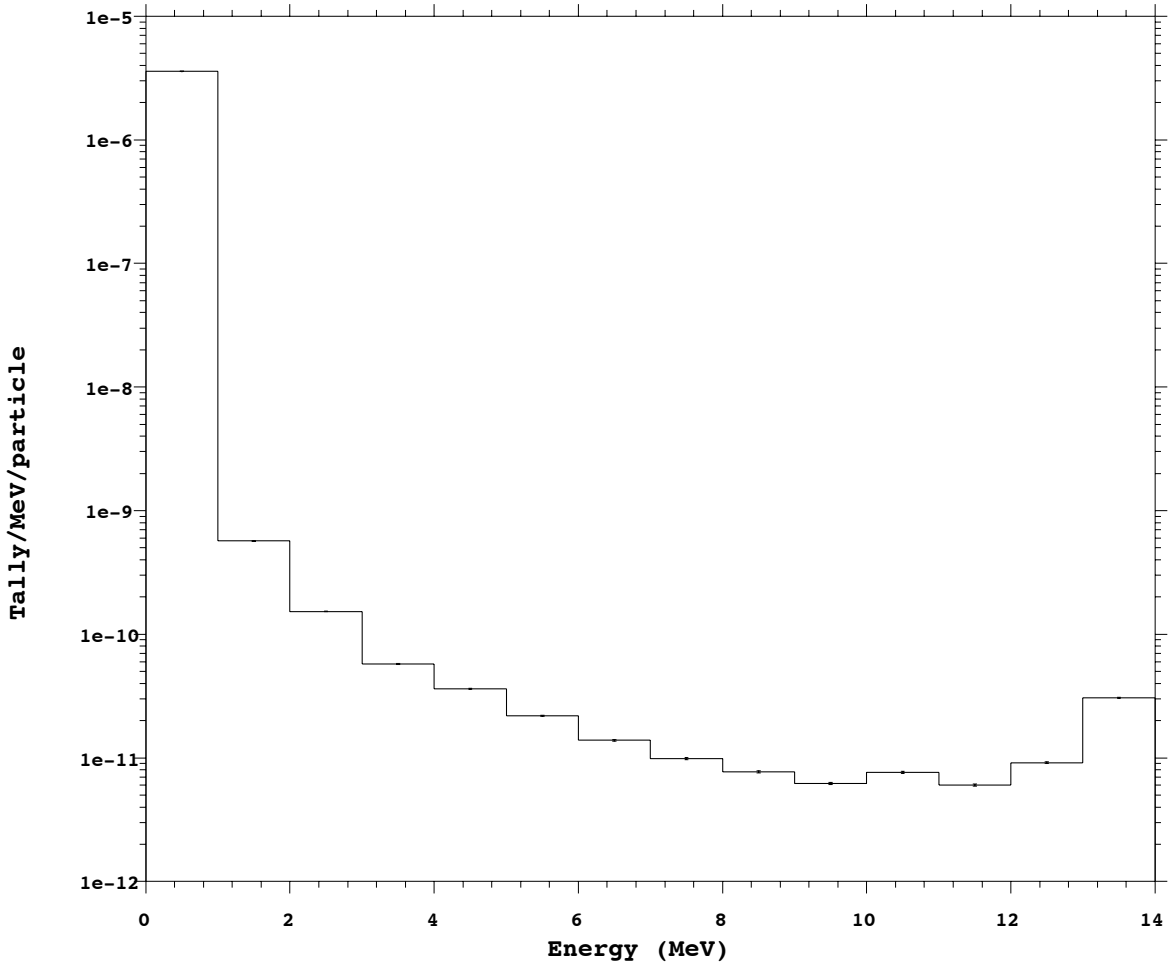

A single-energy 14 MeV neutron source conditioned by propagation through a 3-m-diameter aluminum spacecraft faring.

MCNP Slab Model Results

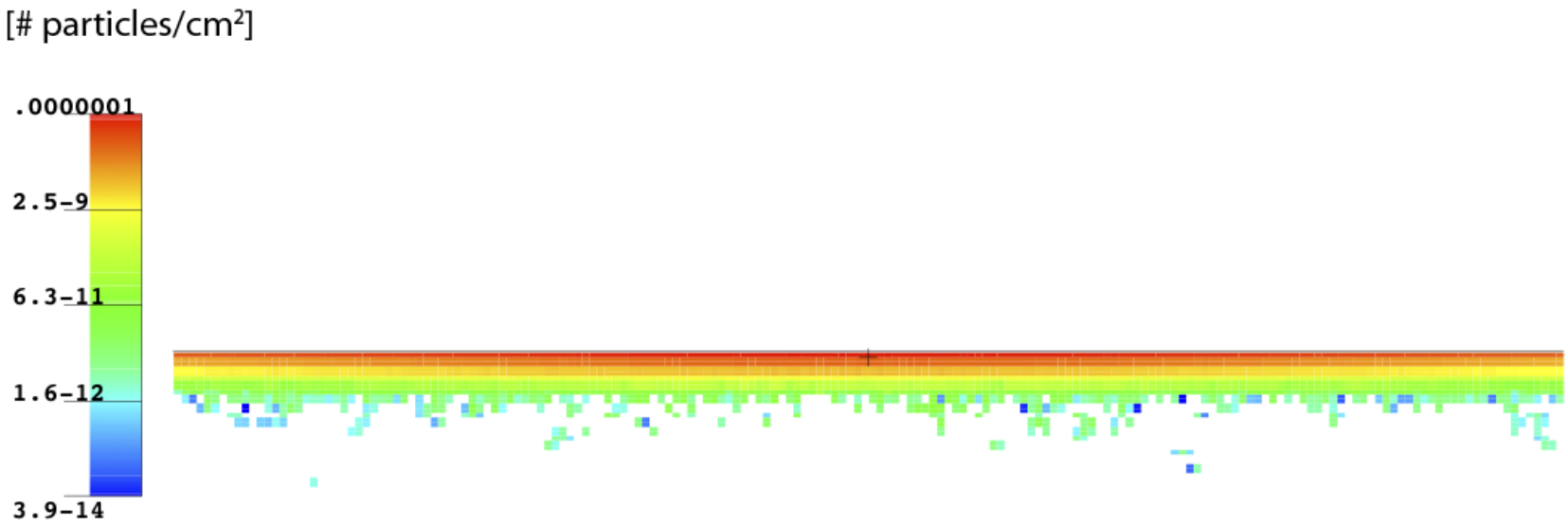

Particle flux through a slab of chondritic material. $\Delta x = 10$ cm

MCNP Slab Model Results

Material	MFP [cm]	Energy [J/kt]	Vapor [g/kt]
Basalt	9.64	2.85×10^7	9.54×10^2
Carbon	2.27	1.31×10^7	1.03×10^3
Chondrite	2.91	4.35×10^7	2.52×10^3
H_2O Ice	0.60	4.01×10^7	1.16×10^4
Iron	33.27	4.22×10^7	5.39×10^3

Units are normalized per kiloton of neutron energy, not total device yield.

Neutron Activation of Meteoritic Material

Would nuclear hazard mitigation include a fallout hazard?

Probably little to none. But we can check.

- Approximate target compositions known
- Common n^0 interactions known
  - inelastic scattering - only energy, momentum transferred
  - absorption, (n,γ)
  - (n,2n)
- Interaction depends on cross-section, n^0 energy, problem geometry, yield
- Interactions tracked in model
- Proxy for daughter isotope production
- Can calculate total production and location

Isotope Production:

$$\text{Production} = (\text{cross section}) \times (\text{atomic fraction of parent})$$

Neutron Activation: CI-Chondrite

- Composition from Lodders (2009)
- 66 different elements
- MCNP model:
  - 14 MeV n^0 source
  - 20-m-diameter target sphere
  - no n^0 escape

Reaction	Daughter Half Life	Daughter production [g/kt]
$^{28}Si(n,d)^{27}Al$	stable	$9.82 \times 10^{-5} \pm 0.003\%$
$^{31}P(n,\gamma)^{32}P$	14.28 days	$4.16 \times 10^{-6} \pm 0.003\%$
$^{56}Fe(n,d)^{55}Mn$	Stable	not predicted
$^{58}Ni(n,d)^{57}Co$	271.79 days	not predicted

Energy Deposition by X-rays

- Gray body radiation: emissivity $\epsilon < 1$
- Vaporized layer thickness:

From the Stefan-Boltzman law:

$$I_{max} < \sigma T_v^4$$

I_{max} = transmitted radiation, energy per unit area,
T_v = vaporization temperature

From the Beer-Lambert law:

$$\Delta y = -\mu ln(I_{max}/I_0)$$

I_0 = incident radiation, μ = permeability

- $\Delta y \approx 1$ mm

The RAGE Hydrocode

- Radiation Adaptive Grid Eulerian
- Gittings et al. (2008)
- Multidimensional simulations
- Adaptive mesh and time steps
- Radiative transfer (grey diffusion), heat conduction
- SESAME and analytical equations of state (EOS)

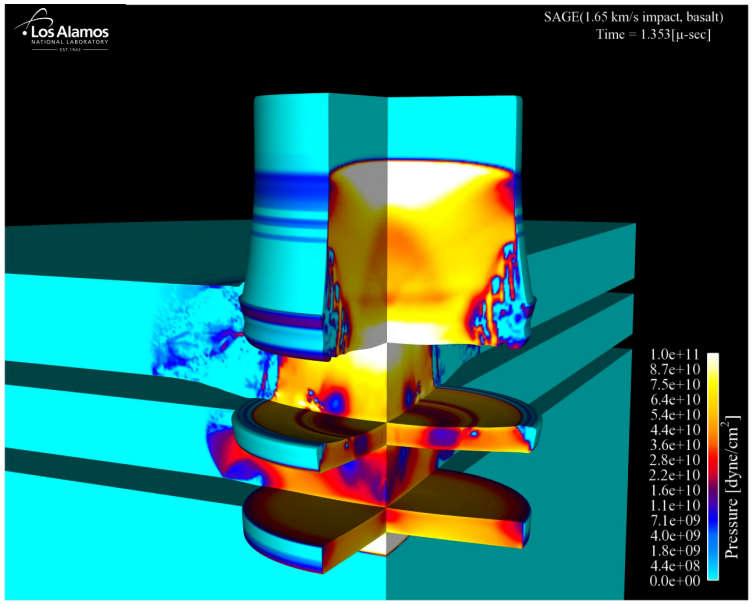

Lab-scale impacts, Plesko (2009).

Stand-Off Bursts and the Effects of Material Properties

- 11-kt burst
- Peak temperature, $T \approx 1$ keV
- 10 m above a planar surface
- SESAME EOS and opacities:
  - H_2O
  - Iron
  - Carbon
  - Basalt
- Simulation goals
  - Explore material property effects
  - Estimate vapor production from x-rays
  - Estimate vapor contribution to momentum

RAGE Slab Model Geometry

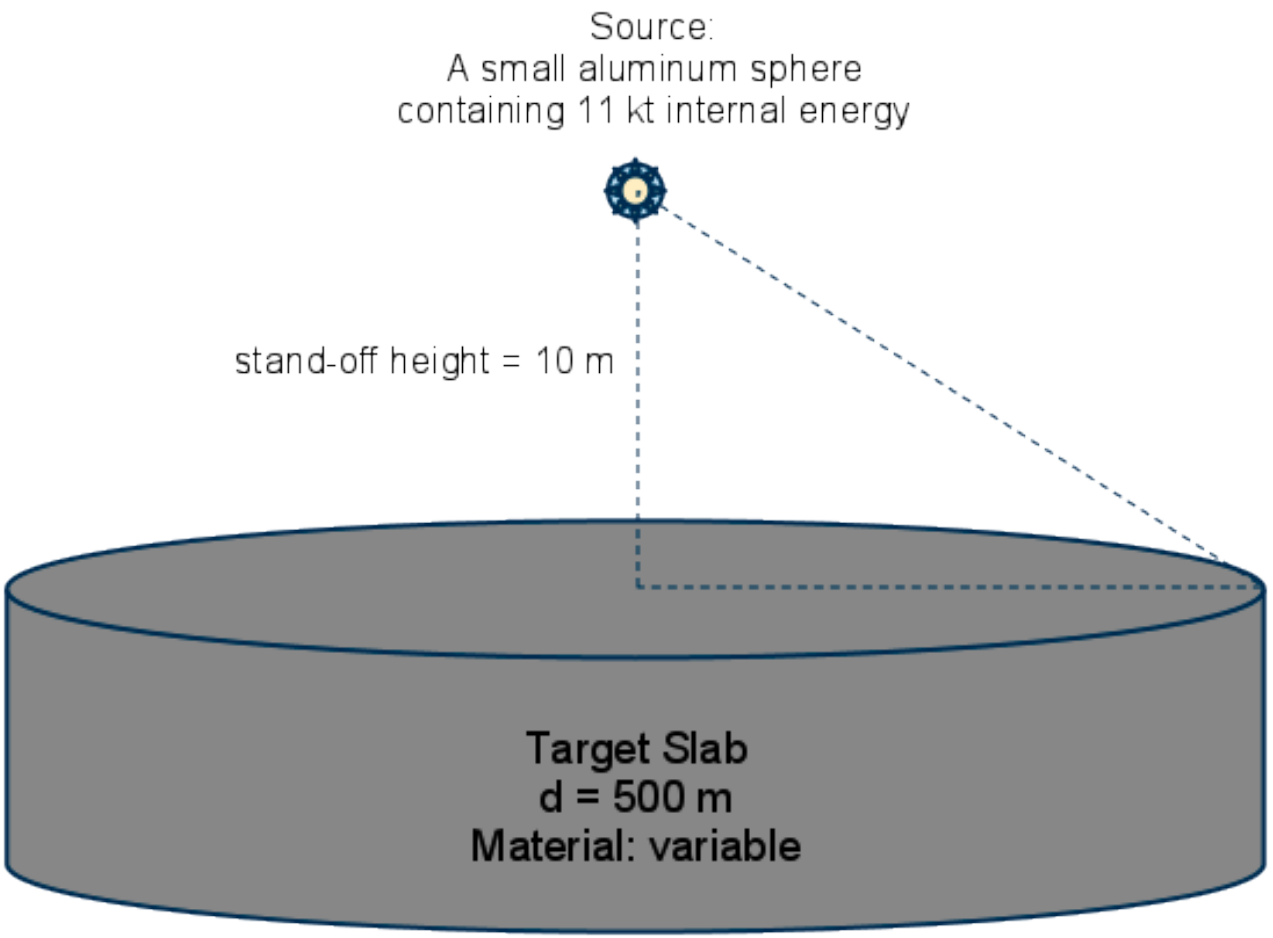

- Mesh resolution: $\delta x = 2.5$ cm

Vapor Production from an 11-kt Stand-Off Burst

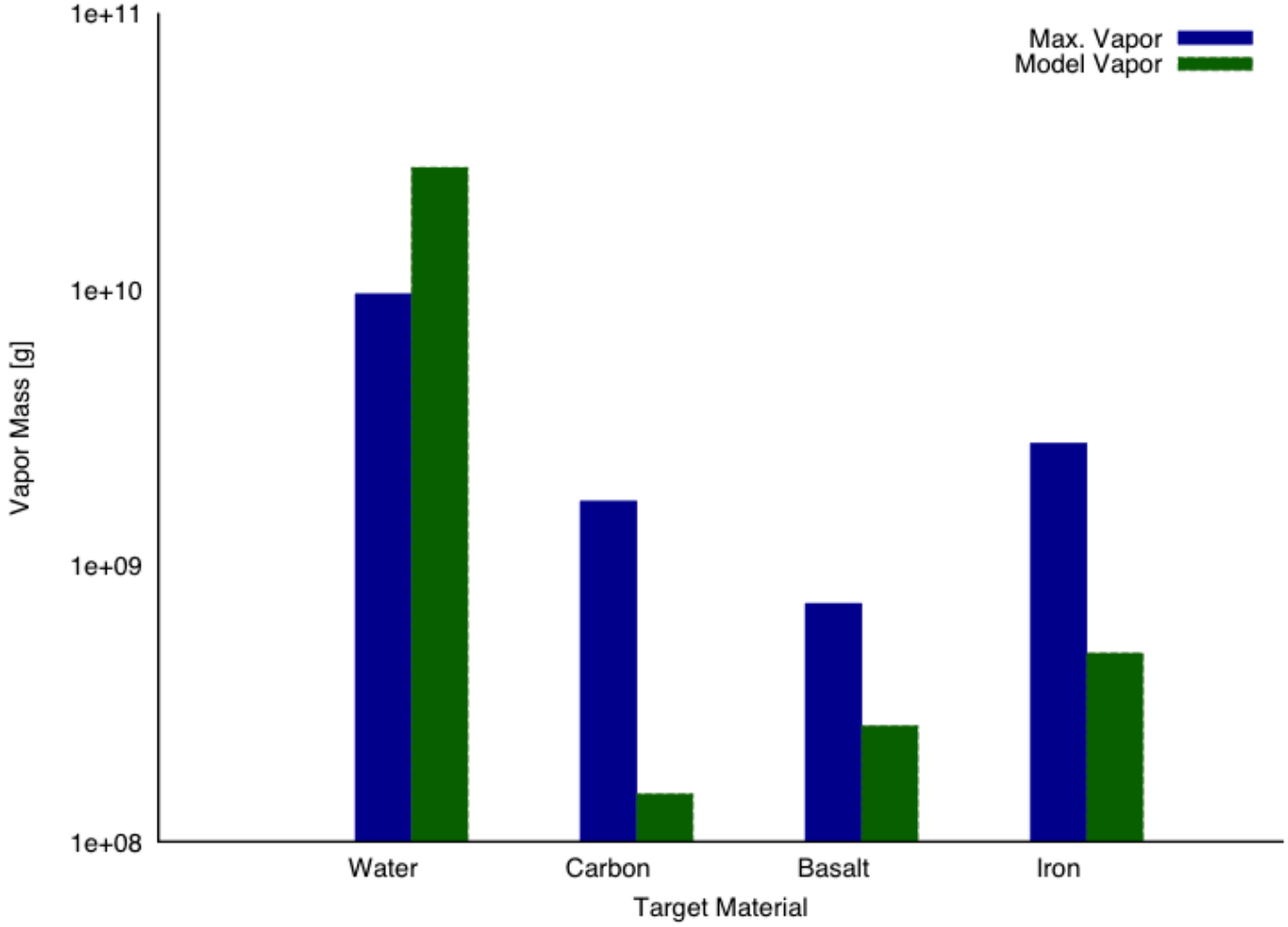

Solid Ejecta From Thermal Expansion and Entrainment

- Ahrens and Harris (1994), Shafer (1994), Holsapple (2004) considered thermal expansion
- Holsapple found thermal expansion ineffective below 60,000 K for porous silicates
- We modeled basalt, $\rho = 1.9$ g/cm^3
- hot layers at T $=$ 600 K, and 11604 K,
- the hot layers were either at the surface, buried disks, or buried boxes.
- above the surface was low-pressure solar wind material

Solid Ejecta From Thermal Expansion

- For buried layers at 600 K, we agree with Holsapple
- Compaction buffers expansion, e.g. Vargas and McCarthy (2007).
- Thermal expansion coefficient small for granular silicates: $\alpha < 0.03$ cm cm^{-1} K^{-1} for granular olivine.
- We see no movement from material at 600 K.

Solid Ejecta From Entrainment in Vapor

- Vacuum enhances vapor production above the liquidus T.
- Buried material at $T > T_l$ still at low P
- Vaporization and decompression can cause blow-off
- $W(\rho, \lambda, g, h)$

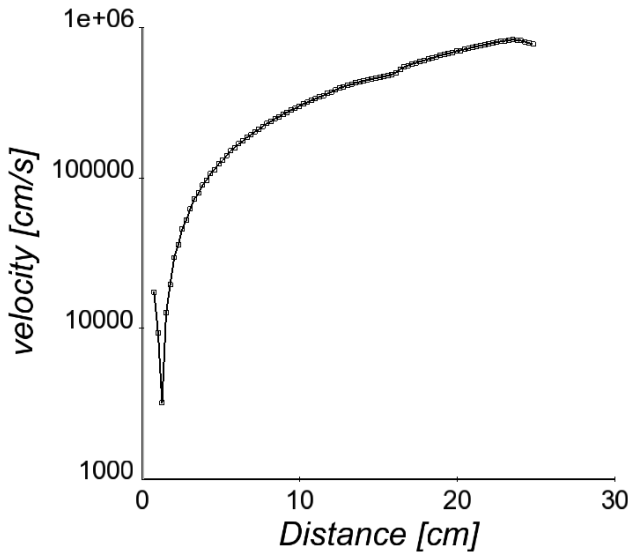

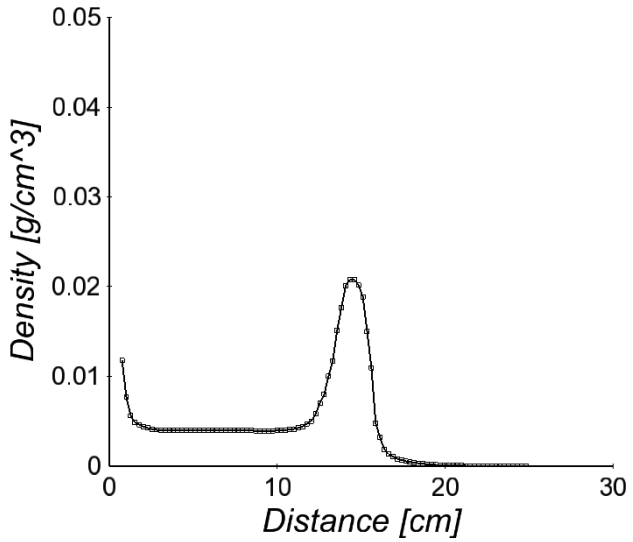

Energy Absorption Results

Material	n^0 MFP [cm]	n^0 E Abs. [J/kt]	x-ray E Abs. [J/kt]
Basalt	9.64	2.85×10^7	1.57×10^{12}
Carbon	2.27	1.31×10^7	8.13×10^{10}
Chondrite	2.91	4.35×10^7	
H_2O Ice	0.60	4.01×10^7	$< 1.89 \times 10^{12}$
Iron	33.27	4.22×10^7	7.6×10^{11}

Energies normalized per kiloton released through each pathway. not device yield.

Vapor Production from an 11-kt nuclear stand-off burst onto a 500-m-diameter slab:

Material	Vapor (x-rays) [g]	Vapor (n^0's) [g]	Total Vapor [g]
Basalt	2.63×10^8	2.14×10^5	2.63×10^8
Carbon	1.49×10^8	1.7×10^5	1.49×10^8
H_2O Ice	2.76×10^{10}	8.68×10^5	2.76×10^{10}
Iron	4.82×10^8	3.18×10^6	4.85×10^8

- Velocities ≈ 10 km/s
- $\Delta p \approx 1.0 \times 10^9$ N·s.

Solid Ejecta

- Compaction buffers thermal expansion of solids.
- Low pressure environment enhances vapor production from melt.
- Energy absorbed at depth from neutrons only matters if it melts.

Conclusions

- Modeled stand-off burst energy deposition
- Vaporization efficiencies $< 30\%$
- Vapor production depends on heat capacity (x-rays), among other things
- Material-specific EOS, opacities, absorption cross sections matter
- EOS data requires experiments, opacities and cross-sections are easier
- Neutron activation calculable, minor, problem dependent
- Vapor contribution from neutrons is minor, $< 1\%$ of total
- May enhance solid ejecta production if buried heated material is vaporized and can escape.